

# Gas Mass Fractions and the Evolution of LSB Dwarf Galaxies

James M. Schombert

Department of Physics, University of Oregon, Eugene, OR 97403; js@abyss.uoregon.edu

Stacy S. McGaugh

Department of Astronomy, University of Maryland, College Park, MD 20742; ssm@astro.umd.edu

Jo Ann Eder

Arecibo Observatory<sup>1</sup>, Puerto Rico, 00612; eder@naic.edu

## ABSTRACT

The optical and HI properties for a sample of low surface brightness (LSB) dwarf galaxies, cataloged from the Second Palomar Sky Survey, is presented. Gas mass fractions for LSB dwarfs reach the highest levels of any known galaxy type ( $f_g = 95\%$ ) confirming that their low stellar densities are due to inefficient conversion of gas mass into stellar mass. Comparison with star formation models indicates that the blue optical colors of LSB dwarfs is not due to low metallicity or recent star formation and can only be explained by a dominant stellar population that is less than 5 Gyrs in mean age. If star formation occurs in OB complexes, similar to normal galaxies, then LSB dwarfs must undergo weak bursts traveling over the extent of the galaxy to maintain their LSB nature, which contributes to their irregular morphological appearance.

*Subject headings:* galaxies: evolution — galaxies: dwarf — galaxies: stellar content

## 1. INTRODUCTION

Dwarf galaxies are important to our understanding of galaxy formation and evolution since they are the smallest sized, star-forming units at the time of galaxy formation. Under the bottom-up scenarios of galaxy formation (Lake 1990, Baugh, Cole & Frenk 1996), dwarf galaxies are the building blocks to the entire Hubble sequence and, thus, the study of dwarf galaxies is a look at the fossil remnants of the early Universe. In addition, dwarfs are extremely rich in dark matter compared to the amount of known baryons calculated from starlight and neutral gas emission (Ashman 1992, Carignan & Purton 1998). They serve as laboratories to test dark matter candidates and the study of the formation and evolution of the dark matter component in galaxies. However, regardless of their cosmological importance, the primary role for dwarf galaxies is that they present us with the extreme limits with respect to star formation and stellar populations in galaxies. Much like the way an abnormal psychologist studies extreme behavior to better understand normal behavior, the study of dwarf galaxies leads to clues into the star formation processes that are found in all galaxies, from dwarf to giant, from quiescent to starburst.

The key to the star formation history of any galaxy, and its subsequent evolution, is its gas supply. Whether the gas supply is converted completely into stars immediately after formation, as in ellipticals, or

---

<sup>1</sup>The Arecibo Observatory is part of the National Astronomy and Ionosphere Center which is operated by Cornell University under contract with the National Science Foundation.

whether the gas supply remains dispersed until a dynamic event increases the number of cloud collisions, as in a tidally induced starburst, the gas mass fraction,  $f_g$ , is the primary parameter for quantifying the evolutionary state of a galaxy. A galaxy's chemical and photometric evolution closely follows the gas consumption rate. For example, Bell & de Jong (2000) demonstrate that the metallicity of spirals follow a simple closed-box chemical evolution model and also predicts the colors of the underlying stellar population. With respect to LSB galaxies, van den Hoek *et al.* (2000) find that a majority of LSB disks can be explained by a exponentially decreasing star formation rate ending with present-day gas fractions near 0.5.

Historically, gas-rich galaxies have divided into two types, disk galaxies and dwarf galaxies. Disk galaxies are brighter and higher in surface brightness and have dominated our studies of the star formation process. In contrast, dwarf galaxies are fainter and lower in surface brightness, making their detection and inclusion in galaxy catalogs problematic. In the last decade, new galaxy catalogs (Schombert & Bothun 1988, Impey *et al.* 1996) have widened our range of central surface brightnesses to include new extremes in low stellar densities (i.e. low surface brightness, LSB). The common interpretation is that these systems have had, in the past, very low rates of star formation (de Blok & van der Hulst 1998) and, thus, there is the expectation that LSB galaxies should be rich in gas compared to their stellar mass. This was confirmed by McGaugh & de Blok (1997, hereafter MdB) in a study of a large sample of disk galaxies over a range of surface brightnesses. They found that there is a strong correlation between a galaxy's gas supply and its stellar density such that galaxies with the lowest surface brightness had the largest  $M_{HI}/L$  and  $f_g$  ratios. The gas fractions found by MdB also indicated that LSB galaxies have the potential to become extremely bright, high surface brightness (HSB) objects if some process increased the efficiency of star formation and rapidly used the supply of gas (e.g. a tidal interaction). The discovery of star-forming dwarf populations in the field (Driver, Windhorst & Griffiths 1995, Schade *et al.* 1996) and in distant clusters (Rakos, Odell & Schombert 1997) makes an investigation into nearby quiescent dwarfs timely.

The correlations found for disk galaxies have never been extended to dwarf galaxies, primarily because of a lack of a uniform sample of gas-rich, LSB dwarfs. The purpose of this paper is undertake a similar analysis performed by MdB on LSB disks to the LSB dwarfs from the PSS-II survey, and to compare the results to the correlations found for all types of disk galaxies. The dwarf sample used herein is based on a visual search of Second Palomar Sky Survey plates (Eder *et al.* 1989, Schombert, Pildis & Eder 1997), parallel to searches for large LSB galaxies (Schombert & Bothun 1988, Schombert *et al.* 1992). This was primarily for a study on biased galaxy formation, but optical and HI data is available for most of the dwarfs. The optical data for that sample was presented in Pildis, Schombert & Eder (1997). The HI data is presented in Eder & Schombert (2000), and forms the core of the analysis in this study.

## 2. OBSERVATIONS

The data for this paper is based on Second Palomar Sky Survey (PSS-II, see Reid *et al.* 1991) plates cataloged in Schombert, Pildis & Eder (1997). The PSS-II differed from the original sky survey in that the latest Kodak IIIa plates, which have greater resolution and depth than the original surveys 103a emulsions ( $250 \text{ lines mm}^{-1}$  versus  $80 \text{ lines mm}^{-1}$ ) were used. The plates used for the dwarf catalog are A or B grade, selected for good surface brightness depth and covering declination zones of the sky that can be observed with the 305m Arecibo radio telescope.

Dwarf candidates from the catalog were observed for the HI line at 21 cm with the Arecibo 305m telescope during the 1992 and 1993 observing season. All observations were made with the 21 cm dual-

circular feed positioned to provide a maximum gain (8 K Jy<sup>-1</sup>) at 1400 MHz. Total velocity coverage of 8000 km s<sup>-1</sup> at a velocity resolution of 8.6 km s<sup>-1</sup> was used. The observations were centered on 4000 km s<sup>-1</sup>, which avoided detection of the strong Galactic hydrogen signal on the low-velocity end, and extended to 8120 km s<sup>-1</sup>. The HI observations are reported in Eder & Schombert (2000).

Successful detections were later selected for follow-up CCD imaging on the Hiltner 2.4m telescope located at Michigan-Dartmouth-M.I.T. (MDM) Observatory. We obtained images using either a Thomson 400 × 576 pixel CCD (0.25 arcsec pixel<sup>-1</sup>) or a Ford-Loral 2048 × 2048 pixel CCD binned 3×3 (0.51 arcsec pixel<sup>-1</sup>), with minimal exposure times of 25 minutes in Johnson *V* and 15 minutes in Johnson *I*. The optical data (luminosities, colors, scale lengths and surface brightnesses) is presented in Pildis, Schombert & Eder 1997).

In addition, data on ordinary spirals was extracted from two surveys, Courteau (1996) and de Jong (1996), for comparison to the LSB dwarf data. The Courteau survey was primarily focused on Sc galaxies, as probes to the Tully-Fisher relation, presenting CCD and HI observations of 189 galaxies. The CCD observations were obtained in *B* and *R*, but a simple linear transformation converts the *R* magnitudes to *I* to match our LSB dwarf luminosities. The de Jong sample consists of a range of spiral types, imaged at *BVRIK*, selected from the UGC with diameters greater than two arcmins and undisturbed in their morphology. HI parameters were obtained from a variety of sources in the literature using NED.

All distance related values in this paper use values of  $H_o = 75$  km sec<sup>-1</sup> Mpc<sup>-1</sup>,  $\Omega_o = 0.2$ , a Virgo central velocity of 977 km sec<sup>-1</sup> and a Virgo infall of 300 km sec<sup>-1</sup>. The data used for this study is available at the LSB dwarf web site (zebu.uoregon.edu/~js).

### 3. DISCUSSION

#### 3.1. Optical Properties

The optical properties of the PSS-II dwarf sample are presented in a previous paper (Pildis, Schombert & Eder 1997). Unless specifically mentioned, all luminosities are *I* band values, scale lengths are measured in *I* band images. The choice of *I* band values is made to minimize the error in calculating stellar mass from optical luminosities. Studies by stellar population models (Worthey 1994) show that  $M_*/L$  varies with time and star formation rate as a function of wavelength, but is most stable in the far-red due to its distance in wavelength from the region around the 4000Å break. Thus, *I* band measurements 1) provide a more accurate estimate of the stellar mass of a galaxy than bluer passbands, 2) obtain a luminosity measure that varies less with recent star formation than bluer passbands and 3) allows determination of structural parameters (such as scale length) which are less distorted by recent star formation events or dust. Although the *I* band is a difficult bandpass to observe, due a bright background from atmospheric OH emission, grey and bright time at many intermediate sized telescopes is much more accessible than dark time, allowing long exposure times at bandpasses where the moonlight has a minor contribution.

To place the LSB dwarf sample in context with respect to disk galaxies, we have selected two comparison samples; the study of regular spirals by de Jong (1996) and a study of Sc galaxies by Courteau (1996). One advantage to using the Courteau Sc disks and de Jong spirals is that both samples were constructed using morphological criteria. The Courteau Sc sample was sorted from the NGC/UGC for late-type galaxies which display clear Sc-type spiral structure and rotational symmetry, specifically to be homogeneous for a study of the Tully-Fisher relation in late-type galaxies. While many of the Courteau objects are low in luminosity and small in size, they are not dwarf-like in their appearance. The de Jong spirals were selected from the

UGC with an emphasis on an undisturbed disk-like appearance and, in this regard, complements Courteau's Sc sample by covering a larger range of disk Hubble types (from Sa to Sm).

The PSS-II dwarf galaxy sample was chosen on two primary characteristics; dwarf-like (i.e. irregular) morphology and low surface brightness (see Schombert, Pildis & Eder 1997). The morphology criteria was introduced to maximize the cataloging of low mass objects to test theories of biased galaxy formation, the original goal of the project, under the assumption that all low mass objects have an irregular appearance. This is not always the case (e.g. dwarf ellipticals), but this criteria has the added advantage of increasing the number of gas-rich dwarf galaxies in the sample and the probability of detection at 21-cm. The low surface brightness nature of the sample is due to the fact that any search for uncataloged galaxies will necessarily be limited by the depth of the survey material. Increased depth does not increase the detection of HSB objects, which are already cataloged unless just below the angular size threshold. The greater sensitivity of the PSS-II plate material produces an automatic bias towards LSB galaxies that were once too diffuse to be visually detected and now have better contrast and, therefore, higher visibility.

In a morphological sense, the de Jong and Courteau samples are diametrically opposite to the PSS-II dwarf sample. Where the disk samples are selected for their regularity in spiral pattern, the LSB dwarfs are selected with an emphasis on their irregularity. The regularity of morphology should be reflecting the star formation history of the galaxy, where a regular pattern in the disk sample evolves from the ordered motions of a density wave and, in contrast, the irregular nature of the LSB dwarfs represents a chaotic history of star formation. Additionally, we can also compare the LSB dwarfs with dwarf sample of Patterson & Thuan (1996, hereafter PT); a sample of galaxies selected from the UGC by morphology in a similar manner to the PSS-II sample and also imaged at  $I$ .

A summary of the optical properties of the four samples is found in Figure 1; histograms of absolute magnitude ( $M_T^I$ ), central surface brightness ( $\mu_o^I$ ) and scale length ( $\alpha$ ). These values are taken directly from Pildis, Schombert & Eder (1997) and MDB. The Courteau Sc sample was converted from  $R$  band data using his  $B - R$  values and a linear extrapolation to  $R - I$  ( $\langle R - I \rangle = 0.5$  for late-type galaxies). Absolute luminosities are based on the total magnitude of the galaxy (integrated curves of growth). Central surface brightness and scale length are based on exponential fits to the surface brightness profiles. Almost all the dwarf galaxies in this sample are well described by an exponential surface brightness profile. For objects with central concentrations (bulge-like cores), the profile fit was made to the linear region only, but the total magnitude includes the core luminosity. Given the extreme late-type nature of the samples, the core contribution is, in any case, very minor.

There are several key points to note from the histograms. One is that there is significant overlap in all of the optical parameters between the four samples. In other words, there is no single property to a galaxy where one could make a division and place dwarfs on one side and ordinary disk galaxies on the other. The de Jong and Courteau samples have similar mean luminosities ( $\langle M_T^I \rangle = -21.2$ ) which is much higher than the LSB or PT dwarf sample ( $\langle M_T^I \rangle = -17.4$ ). This is not surprising since spiral galaxies are known to have high rates of star formation, often covering most of their disk area, resulting in more stellar mass and, therefore, higher central surface brightnesses. Surface brightness is not directly correlated with total luminosity, as can be seen from the distribution of the de Jong disk total magnitudes (see also Driver & Cross 2000). The LSB dwarf sample displays a fairly sharp cutoff in luminosity at  $M_T^I = -19$ , despite the fact that only morphology and surface brightness were used to select the sample.

The trend of central surface brightness in each sample is as expected. The LSB dwarfs have a low mean central surface brightness ( $\langle \mu_o \rangle = 21.8$ ), although the de Jong disk sample overlaps the LSB dwarf sample

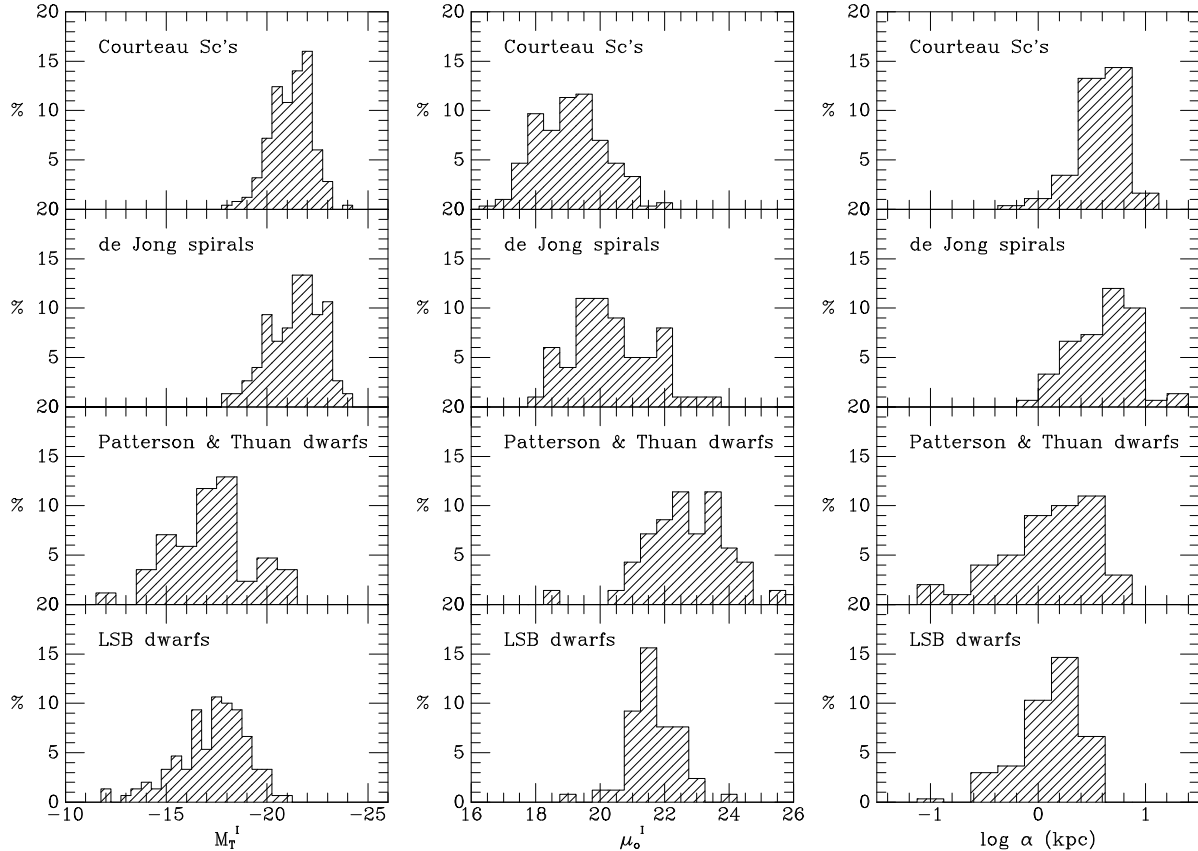


Fig. 1.— Histograms of total luminosity ( $M_T^I$ ), central surface brightness ( $\mu_o^I$ ) and scale length ( $\alpha$ ) for the Courteau sample of Sc galaxies, de Jong sample of ordinary spirals, Patterson and Thuan UGC dwarf sample and the LSB dwarf sample. The LSB dwarfs define a low luminosity, low surface brightness and small scale length sample of galaxies.

(there are several Sd and Sm class spirals in the de Jong sample). The PT dwarf sample has a similar distribution with a slightly fainter mean  $\mu_o$ . The Courteau Sc sample has a brighter mean  $\mu_o$  ( $\langle \mu_o \rangle = 19.0$ ), but the range is quite broad.

The histograms of scale length,  $\alpha$ , are intriguing in that the de Jong disk and Courteau Sc sample have identical distributions despite having reached their optical appearances by very different star formation histories (based on the final morphology and central surface brightness). This leads us to conclude disk galaxies have the same range of sizes and masses and Hubble class is imposed on disk galaxy structure by a set of parameters only weakly linked to the structural ones (angular momentum, environment, etc, see Zaritsky 1993). The LSB and PT dwarfs have much lower values of  $\alpha$  with a cutoff at 3 kpc. In fact, the size distribution is perhaps the most accurate method of distinguishing dwarf from ordinary galaxies when the mass is unknown (see Schombert *et al.* 1995).

### 3.2. HI Properties

It is often stated that LSB galaxies are gas-rich, which is loosely defined to mean that they have high amounts of neutral hydrogen compared to their optical luminosities. It should be noted that to state that the LSB dwarf sample is gas-rich does not imply that they have high HI masses. The distribution of HI masses (calculated from the total HI flux using the prescription of Giovanelli & Haynes 1988) is shown in Figure 2 along with the HI mass distribution of the de Jong spiral, Courteau Sc and PT dwarf samples. The LSB dwarf distribution has a low mean value ( $\langle M_{HI} \rangle = 10^9 M_\odot$  compared to the  $\langle M_{HI} \rangle = 8 \times 10^9 M_\odot$  for the disk samples) with a long tail towards low HI masses. It is important to note that dwarfs selected by optical characteristics, such as size, are also dwarfs in terms of HI mass (see Eder & Schombert 2000).

The dwarfs in Figure 2 with HI masses less than  $10^8 M_\odot$  are of interest to galaxy population studies since there is some suggestion of a steeping of the HI mass function below  $10^7 M_\odot$  (Schneider, Spitzak & Rosenberg 1998, Zwaan *et al.* 1997). There is no correlation between HI mass and surface brightness (Pildis, Schombert & Eder 1997); however, none of the  $M_{HI} < 10^8 M_\odot$  dwarfs have central surface brightnesses brighter than  $\mu_o^I = 21$  (approximately  $\mu_o^B = 22.5$ ). This implies that low HI mass objects are under represented in our catalogs, because of their bias towards high surface brightnesses objects, and LSB, low HI mass galaxies have gone undetected in optical surveys (Schneider & Schombert 2000).

The distribution of the HI mass to luminosity ratio ( $M_{HI}/L$ ) is shown in the middle panel of Figure 2. The disk samples cover the same range (from  $M_{HI}/L = 0.03$  to 5); however, the Sc sample has a slightly higher mean ( $\langle M_{HI}/L \rangle = 0.8$ ) than the de Jong spirals reflecting the known dependence of  $M_{HI}/L$  on Hubble type. The LSB dwarf sample has the highest mean of  $M_{HI}/L$  values ( $\langle M_{HI}/L \rangle = 3$ ), reflecting the increasing importance of neutral hydrogen to the baryonic content of these galaxies (see discussion in §3.4). Matthews, van Driel & Gallagher (1997) isolated a similar sample of high  $M_{HI}/L$  galaxies, also selected from late-type galaxies, and the LSB dwarf sample share many of the same characteristics with their galaxies.

The relationship between stellar mass and gas mass is shown in Figure 3. As discussed in §3.1, the luminosity of a galaxy at 9000Å is an excellent measure of the number of stars in a galaxy since star formation effects dominate in the blue portion of the spectrum. To determine the stellar mass of a galaxy, we require the mass to light ratio,  $\Upsilon_*$ . Ideally, we would like to measure  $\Upsilon_*$  directly by some dynamical means such as the observations of the vertical stellar velocity dispersion (Bottema 1993). Lacking such detailed information for each galaxy, we follow the work outlined in MdB and de Jong (1996). Based on dynamical data and stellar population models (Bruzual & Charlot 1993), they determine that there is a

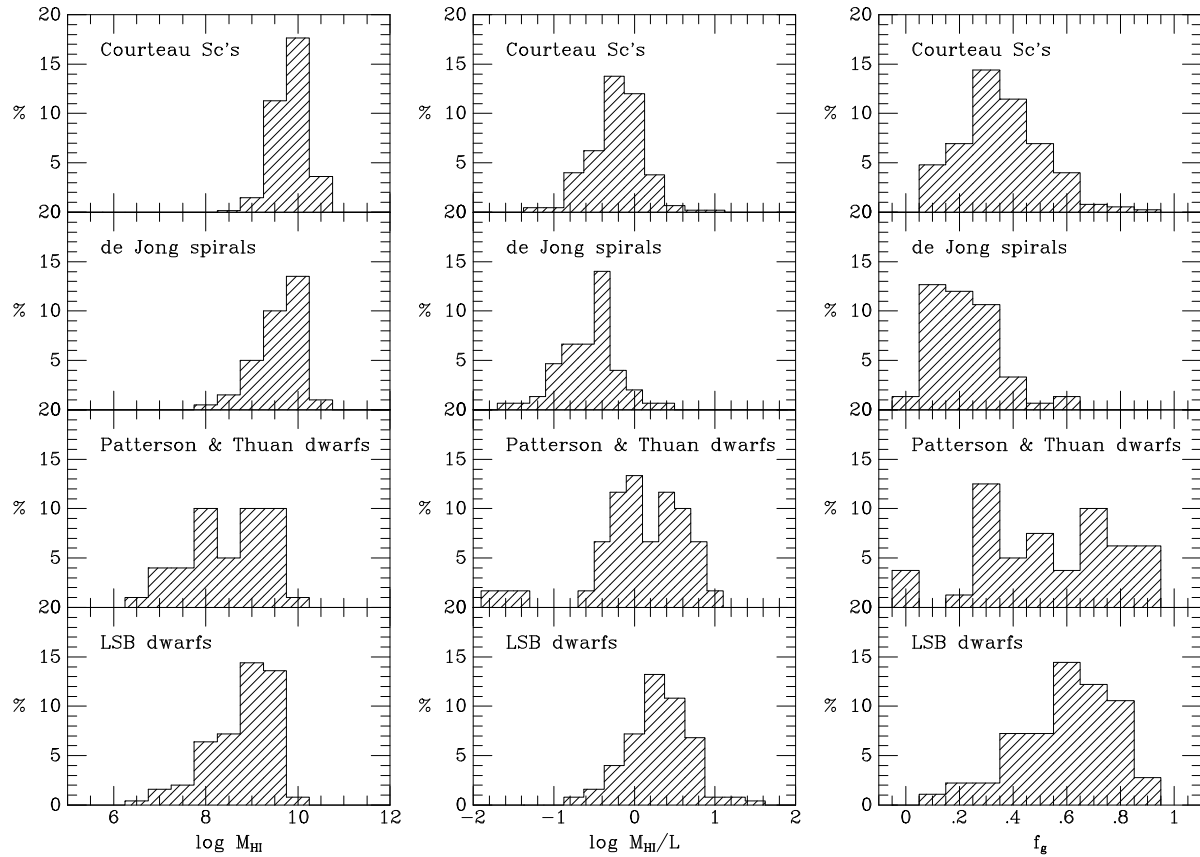


Fig. 2.— Histograms of HI mass, HI mass to light ratio ( $M_{HI}/L$ ) and gas mass fraction ( $f_g$ ). While LSB dwarfs are low in total gas mass, their gas fractions are much higher than the spirals samples.

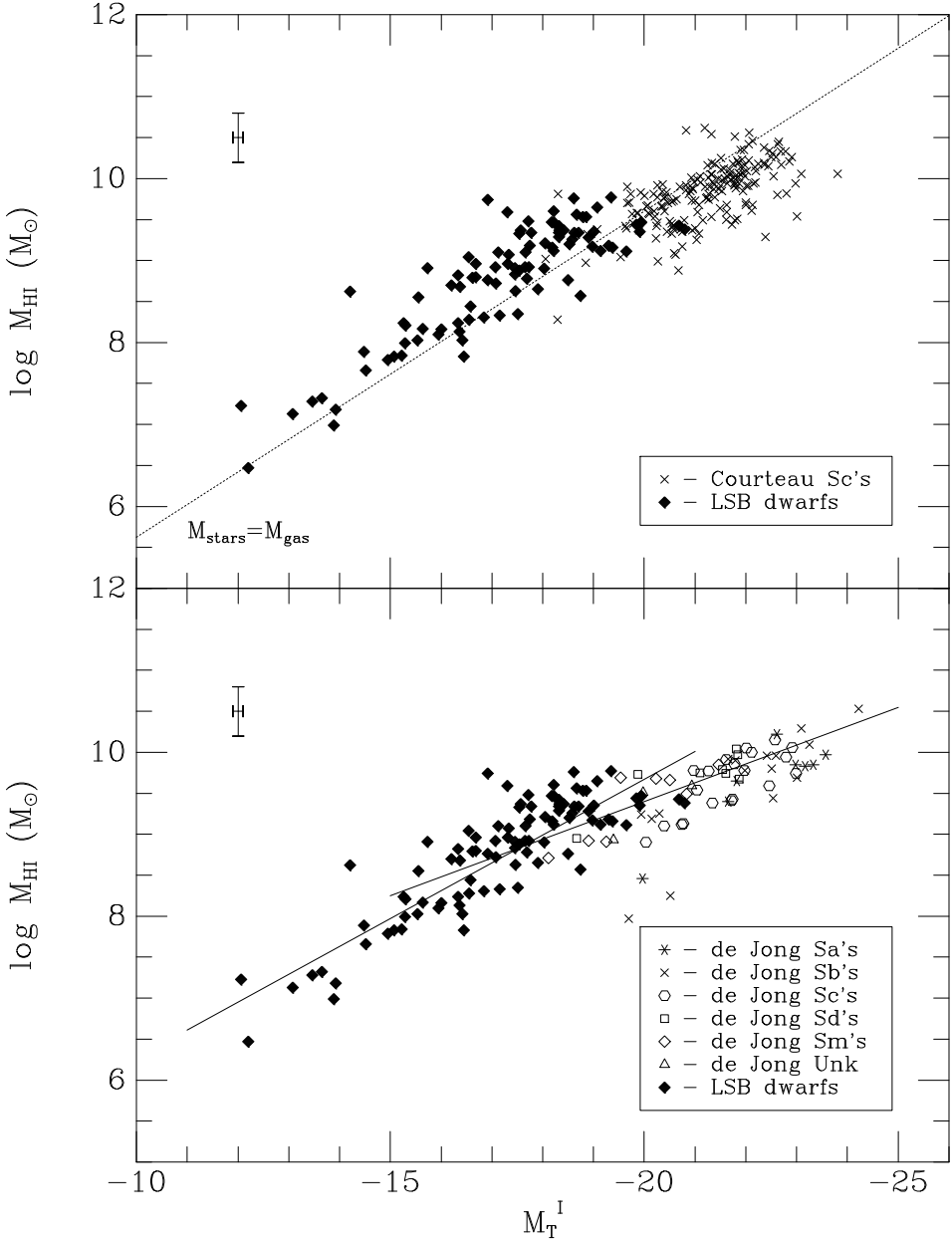


Fig. 3.— Total luminosity versus HI gas mass for LSB dwarfs compared to Courteau Sc's (top panel) and de Jong spirals (bottom panel). The line of equal gas and stellar mass (assuming an  $M_*/L$  of 1.7 (McGaugh *et al.* 2000) and a conversion of HI to gas mass of 1.4) is shown in the top panel. The ordinary spirals display a shallower slope in the gas to stellar relationship, indicating that LSB dwarfs have been inefficient at converting their gas into stars.

factor of two spread in  $\Upsilon_*$  in the  $B$  bandpass, but that in  $I$  there is only a modest variation (less than 10%). Following the analysis presented in de Jong (1996), we adopt a mean value of  $\Upsilon_*=1.7$ , although we note that a recent set of spectroevolutionary models by Bell & de Jong (2001) suggest that  $M/L$  can vary as much as a factor of 2 over the color range of the dwarfs presented herein (see their Figure 3).

The Courteau Sc sample is plotted with the LSB dwarfs in the top panel, the de Jong spiral sample is plotted in the bottom panel. Also shown in the top panel is the equality line for gas and stellar mass, where the gas mass is determined from the HI mass after corrections for metals and non-atomic gas (see §3.4). There has been no detection of CO emission from any LSB galaxy (Schombert *et al.* 1990, de Blok & van der Hulst 1998), so corrections for molecular gas are considered to be negligible (see Mihos, Spaans & McGaugh 1999). For a majority of the disk galaxies in the de Jong and Courteau samples, the baryonic matter is in the form of stars since their data points lie below the  $M_{stars} = M_{gas}$  unity line. The opposite is true of the dwarfs, where a significant fraction of their baryonic matter is in the form of gas (primarily neutral hydrogen). Thus, the term ‘gas-rich’ dwarf refers to this reversal of stellar mass dominance in disk galaxies to gas mass dominance for the dwarf sequence.

The correlation between HI mass and total luminosity is not linear (in log space, i.e. different power law slopes) for the whole range of galaxy luminosities. In fact, the dwarf sequence clearly has a steeper slope than both the de Jong spiral and the Courteau Sc sample. Linear fits to the three samples produce the following relations:

$$\begin{aligned}\log M_{HI} &= -0.22M_T^I + 5.16 \text{ (Courteau Sc's)} \\ \log M_{HI} &= -0.23M_T^I + 4.80 \text{ (de Jong disks)} \\ \log M_{HI} &= -0.34M_T^I + 2.87 \text{ (LSB dwarfs)}\end{aligned}$$

where the fits to the disks and dwarfs are shown in the bottom panel of Figure 3. The error on the slopes is  $\pm 0.02$ . The de Jong spirals are slightly more gas massive than the Sc sample at the low luminosity end, in agreement with the findings of de Blok, McGaugh & van der Hulst (1996). Some adjustment might be necessary to the Sc sample since they contain a small fraction of their gas in molecular form (although this amount is very small, see Young and Knezek 1989).

Assuming that  $M_*/L$  does not systematically change with  $M_{gas}$  between late-type disks and dwarfs, the relation between stellar and gas mass is given by:

$$\begin{aligned}M_{gas} &\propto M_*^{0.55} \text{ (disks)} \\ M_{gas} &\propto M_*^{0.88} \text{ (dwarfs)}\end{aligned}$$

The shallower slope for disk galaxies implies that they have been more efficient at converting gas into stars in the past, assuming that all galaxies form from a single reservoir of gas. This also agrees with the previous observation that disk galaxies typically have a greater amount of their baryonic mass in stars rather than gas. Interestingly, even the LSB spirals in de Jong’s sample, which have different star formation histories from other spirals in the sample, display the same gas to stellar mass behavior as the Sc galaxies.

### 3.3. Gas Fractions

The standard measure of the gas-richness of a galaxy is their ratio of the gas mass to the luminosity,  $M_{HI}/L$ . Figure 2 displays the distribution of  $M_{HI}/L$  for dwarfs versus the two spiral samples. The LSB dwarf sample has a higher mean  $M_{HI}/L$  (5 versus 1/2 for disks), but there is a great deal of overlap between the samples. Note that many LSB dwarfs presented herein have  $M_{HI}/L$  values greater than 5. This represents new extremes in gas to light ratio since, for example, none of the dwarfs studied by either van den Hoek *et al.* (2000) or van Zee, Haynes & Salzer (1997) have  $M_{HI}/L$  values above 0.5 at  $I$ . More relevant is the trend of  $M_{HI}/L$  with luminosity (i.e. stellar mass) and central surface brightness (i.e. stellar density). These diagrams are shown in Figure 4 for the LSB dwarf and de Jong spiral sample. Where the trend for higher  $M_{HI}/L$  with lower luminosity in the de Jong disk galaxies continues to lower luminosities, the dwarf data, by itself, is not as highly correlated as the disk galaxies.

The change in the relationship between  $M_{HI}/L$  and central surface brightness ( $\mu_o^I$ ) is particularly striking from the disks to dwarfs (top panel of Figure 4). The previously tight correlation for ordinary spirals all but disappears for the dwarfs. However, the dwarfs do serve to fill the high  $M_{HI}/L$ , low  $\mu_o^I$  region of the diagram. In fact, the previous correlations may be mostly due to various boundary conditions imposed by our galaxy catalogs and unfilled regions of the diagram which are empty for astrophysical reasons. For example, the sharp lower boundary may mark the limit placed by galactic winds from the first epoch of star formation. As the surface density of a galaxy drops (i.e. lower surface brightness), it becomes easier to eject its ISM due to heating by SN (Dekel & Silk 1986). Thus, the lower left region of the  $M_{HI}/L - \mu_o^I$  diagram would be inhabited by objects with neither sufficient gas (due to blowout) nor stars (due to a lack of gas for star formation) to be detected in the optical or radio (e.g., extremely LSB dwarf ellipticals). On the other hand, the upper right region of the diagram is an area that would be occupied by extremely bright, high HI mass galaxies. Such objects are expected to be short-lived as it would be unstable to strong star formation events, converting all its gas into stars and, thereby, rapidly lowering its  $M_{HI}/L$  value.

The  $M_{HI}/L$  values can also be used to determine the gas fraction in a galaxy. As outlined by MDB, the baryonic gas mass fraction is given by

$$f_g = \frac{M_g}{M_g + M_*}$$

where  $M_g$  is the total mass in the form of gas (neutral, ionized and metals), and  $M_*$  is the mass in stars. To relate these to the HI observations, we need the stellar mass to light ratio ( $M_* = \Upsilon_* L$ ) and the amount of gas represented by neutral hydrogen ( $M_g = \eta M_{HI}$ ). The parameter  $\eta$  plays an analogous role for the gas as  $\Upsilon_*$  does for stars and accounts for both helium, metals and for gas phases other than atomic hydrogen. With these definitions, it is straight forward to obtain

$$f_g = \left( 1 + \frac{\Upsilon_* L}{\eta M_{HI}} \right)^{-1}.$$

Again, following the analysis presented in McGaugh *et al.* (2000), we adopt their mean value of  $\Upsilon_* = 1.7$ .

For the gas,  $\eta$  must be corrected for both the hydrogen mass fraction  $X$ , and the phases of gas other than atomic. We assume a solar hydrogen mass fraction, giving  $\eta = X_{\odot}^{-1} = 1.4$ . Variations in helium and metal content result in deviations from this value of less than 10%. This is a very small effect compared to that of other gas phases. Ionized gas in HII regions and hotter plasma is of negligible mass in late-type

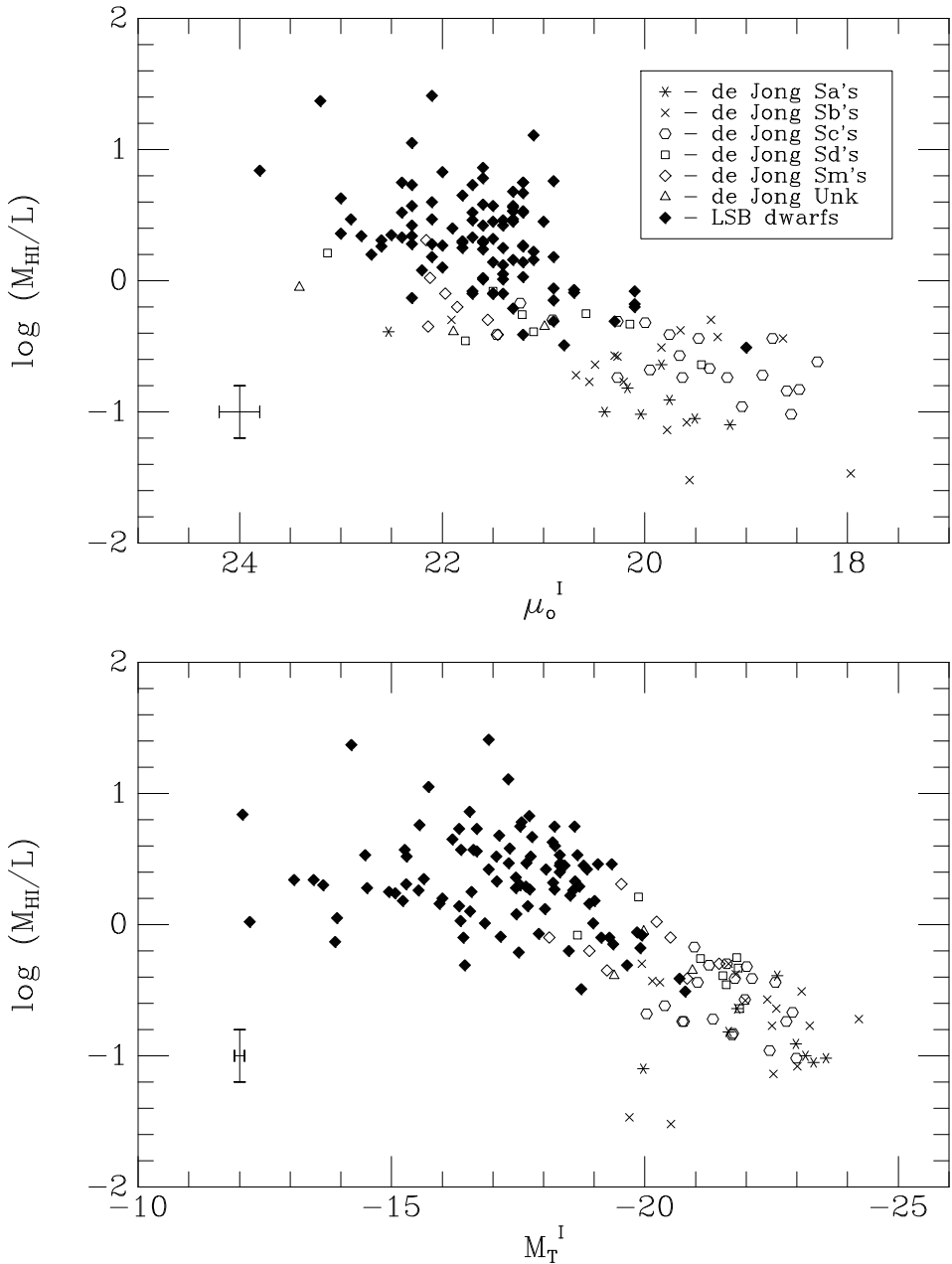


Fig. 4.— Gas to light ratios ( $M_{HI}/L$ ) versus total luminosity and surface brightness. The previously strong correlations for disk galaxies is extended by LSB dwarfs, but the LSB dwarfs are not as well-correlated by themselves.

galaxies. In addition, molecular gas is also negligible for galaxy types later than Sc (Young & Knezek 1989) and there has been no detectable CO emission in LSB galaxies (Schombert *et al.* 1990). Therefore, we adopt the solar hydrogen mass fraction of 1.4 for  $\eta$ .

The histograms of gas fraction,  $f_g$ , for the LSB dwarf and comparison disk samples are shown in Figure 2. The gas fractions display similar behavior to the HI mass distributions. A majority of the galaxies in the disk samples have  $f_g$  values below 0.5; whereas, the dwarf galaxies have very high  $f_g$  values, many objects reaching an unprecedented 90% in gas fraction. In the disk samples, the  $f_g$  values peaked at 0.3, but in the dwarf sample over 90% of the galaxies have  $f_g$  greater than 0.3. Note that the high  $f_g$  values for LSB dwarfs implies that there has been no epoch of baryonic blowout such as has been found for early-type galaxies (Bothun, Eriksen & Schombert 1994, MacLow & Ferrara 1999) unless there has been gas replenishment by infall, an unlikely prospect given the low dynamical masses of these systems (Eder & Schombert 2000). Adjusting the  $\Upsilon_*$  for the bluer colors of LSB dwarfs would increase, on average, the calculated  $f_g$  making their distribution even more extreme compared to disks.

The relationship between gas fraction and the optical properties of a dwarf galaxy are not as strong as those for disk galaxies, but several trends are clear. Lower luminosity and low surface brightness (lower stellar density) dwarf galaxies have much higher gas fractions than disk galaxies. Most dwarfs have higher gas fractions than either HSB or LSB disk galaxies (see MdB Figure 8), yet lack the strong correlation with luminosity or surface brightness that suggests a less orderly star formation history compared to disks. We interpret this trend to imply that LSB dwarfs are LSB simply because they have not converted their gas into stars at the same efficiency as either HSB or LSB disks.

To investigate this behavior further, we have adapted the chemical and spectrophotometric model from Boissier & Prantzos (2000, hereafter BP) which present predictions of gas fractions, surface brightness and color for a range of galaxy masses. While intended to model disk galaxies, the BP models follow a CDM framework and use scaling laws (Mo, Mao & White 1998) that should be applicable to dwarf galaxies as well as disks. The smallest masses in their models correspond to rotation values of 80 km/s, which is similar to the HI widths of the LSB dwarf sample.

A full description of the BP models can be found in their series of papers (see BP for references). Briefly, the models assemble a set of evolving rings to represent a galaxy formed by primordial infall. The CDM scenario for galaxy formation requires the density fluctuations in the early Universe give rise to dark matter dominated halos. Within these halos, baryonic gas condenses to form disks. The resulting disks will have characteristic central densities, scale lengths and masses in scalable terms, although not necessarily correlated since a galaxy of a particular mass can form with a range of central surface brightnesses and sizes. In order to distinguish various models, BP introduce the spin parameter,  $\lambda$ , relating halo mass and angular momentum as described by Mo, Mao & White (1998), as the fundamental parameter to characterize the models.

Under this formalism, the spin parameter and circular velocity (effectively, the disk mass) determine the characteristic timescale for star formation. In addition, the model galaxy's structure are such that low  $\lambda$  models ( $\lambda=0.01$ ) simulate HSB galaxies and high  $\lambda$  models ( $\lambda=0.09$ ) have surface brightness profiles that recover that same structure as LSB dwarfs and disks. The simulations also allow the tracking of gas and stellar mass fractions as a function of time. By late epochs (13 Gyrs, see BP Figure 8), high  $\lambda$  simulations have gas fractions between 0.6 and 0.8, similar to the values found for the LSB dwarfs in our sample. All this formalism is normalized to data for the Milky Way, thus completing the circle of structural and stellar population effects.

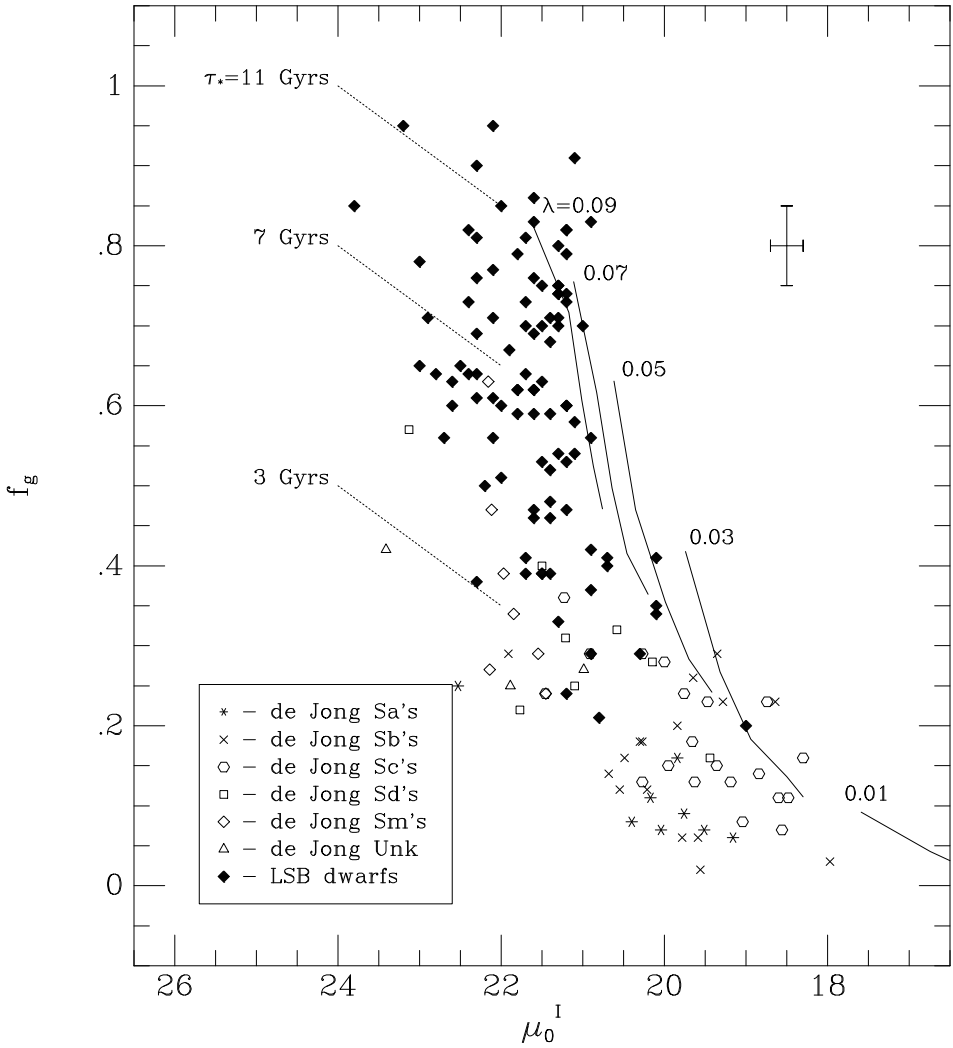


Fig. 5.— Central surface brightness ( $\mu_0^I$ ) versus gas mass fraction ( $f_g$ ). The data from de Jong for disk systems is shown by morphological type. LSB dwarfs (solid diamonds) are, typically, much higher in gas fraction. Also shown are the 13 Gyr galaxy evolution models of Boissier & Prantzos (2000). Each solid track follows the model gas fraction and surface brightness as a function of mass for various spin parameters,  $\lambda$ . High  $\lambda$  values correspond to LSB systems, low  $\lambda$  values scale to normal disk galaxies. Lower  $f_g$  values on each track indicate the higher mass models, opposite edge are for galaxies with circular velocities of 80 km/s. While the models predict the observed  $f_g$  values for LSB dwarfs, the model surface brightnesses are between 0.5 and 1 mags too bright. Under the model formalism, this would imply ages for the LSB dwarfs of 3 to 5 Gyrs younger than the shown models. Also shown are tracks of e-folding star formation timescales (dotted lines) from the evolution models. LSB dwarfs display longer star formation timescales than disk systems.

A comparison of the BP models (at timestep 13 Gyrs) and the LSB dwarf gas fractions and surface brightnesses is found in Figure 5. Each set of models for a specific spin parameter,  $\lambda$ , cover a range of gas fractions and central surface brightness. Each track represents a single values of  $\lambda$ , where the brighter (lower  $f_g$ ) edge of the tracks represent high mass (high  $V_c$ ) models and the fainter edge corresponds to low mass systems. As can be seen in Figure 5, the BP models predict the general trend of higher  $f_g$  with fainter  $\mu_o$ . However, the models appears to be about one magnitude too bright compared to the position of the LSB dwarfs and disks.

A similar disagreement between models and observations was noted in BP for the low surface brightness realm and it seems clear that additional models with  $\lambda > 0.1$  would begin to match the observed central surface brightnesses of LSB dwarfs. However, we also note that age could also explain the discrepancy between the models and observations. The low mass, high  $\lambda$  models typically brighten by one magnitude between 7 and 13 Gyrs (due to an increasing SFR and continued conversion of gas mass into stellar mass). Thus, if LSB dwarfs were, on average, 5 Gyrs younger than other disk galaxies then the models would exactly match the data. Color information confirms this interpretation as will be discussed in the next section. Since the lower  $\lambda$  models require decreasing star formation rates, then the surface brightness offset seen between the models and the disk data is probably due to a mismatch in the models to the accumulation of stellar mass relative to the Milky Way. Younger age is not an explanation for the disk systems since a decreasing star formation leads to a fading in surface brightness, opposite to what is seen in Figure 5.

The various  $\lambda$  models also map into star formation e-folding times (as given by Figure 5 in BP) as a function of galaxy mass. Boundaries for star formation timescales of 11, 7 and 3 Gyrs are also shown in Figure 5. As one would expect from their high gas fractions, LSB dwarfs typically lie in the region of the diagram occupied by galaxies with very long e-folding timescales. This would agree with their low metallicity values (McGaugh 1994, van Zee, Haynes & Salzer 1997) and the low current star formation rates, based on H $\alpha$  imaging, and support the conclusion that LSB dwarfs are slowly evolving systems.

### 3.4. Colors

The final clue to the star formation history of LSB dwarfs lies in their colors. Figure 6 displays the  $V - I$  colors versus total luminosity ( $M_T^I$ ), central surface brightness ( $\mu_o^I$ ) and gas fraction ( $f_g$ ) for the LSB dwarfs and de Jong spirals.  $V - I$  is chosen as the comparison color since it focuses on the mean color of the giant stars in a galaxy, a measure of the star formation in the last 5 Gyr, rather than a color index such as  $B - V$ , which is a measure of contribution from massive stars (i.e. very recent star formation). This is an important distinction since interpretation using the  $V - I$  colors can not discriminate between constant star formation over 5 Gyrs or a series of short, weak bursts within that same time frame.

Several familiar trends are evident from Figure 6. One is that there is a clear tendency for galaxies to have bluer colors with lower surface brightness (middle panel, Figure 6). This pattern was first noticed by Schombert *et al.* (1992), and has been studied by several authors (Gerritsen and de Blok 1999, Bell *et al.* 2000). Blue optical colors were of early importance since they eliminated the fading hypothesis for the evolution of LSB galaxies (McGaugh & Bothun 1994, see O’Neil *et al.* 1997 for the discovery of red LSB galaxies). It is interesting to note that the scatter in the color diagrams is much less at  $I$  versus the same diagrams using  $B$  or  $V$  magnitudes (see McGaugh, Schombert & Bothun 1997). This is due to the fact that LSB galaxies, by definition, have low luminosity densities so that the contrast of recent star formation is extremely sharp in blue indices, whereas the comparison of colors in the far-red tends to average color

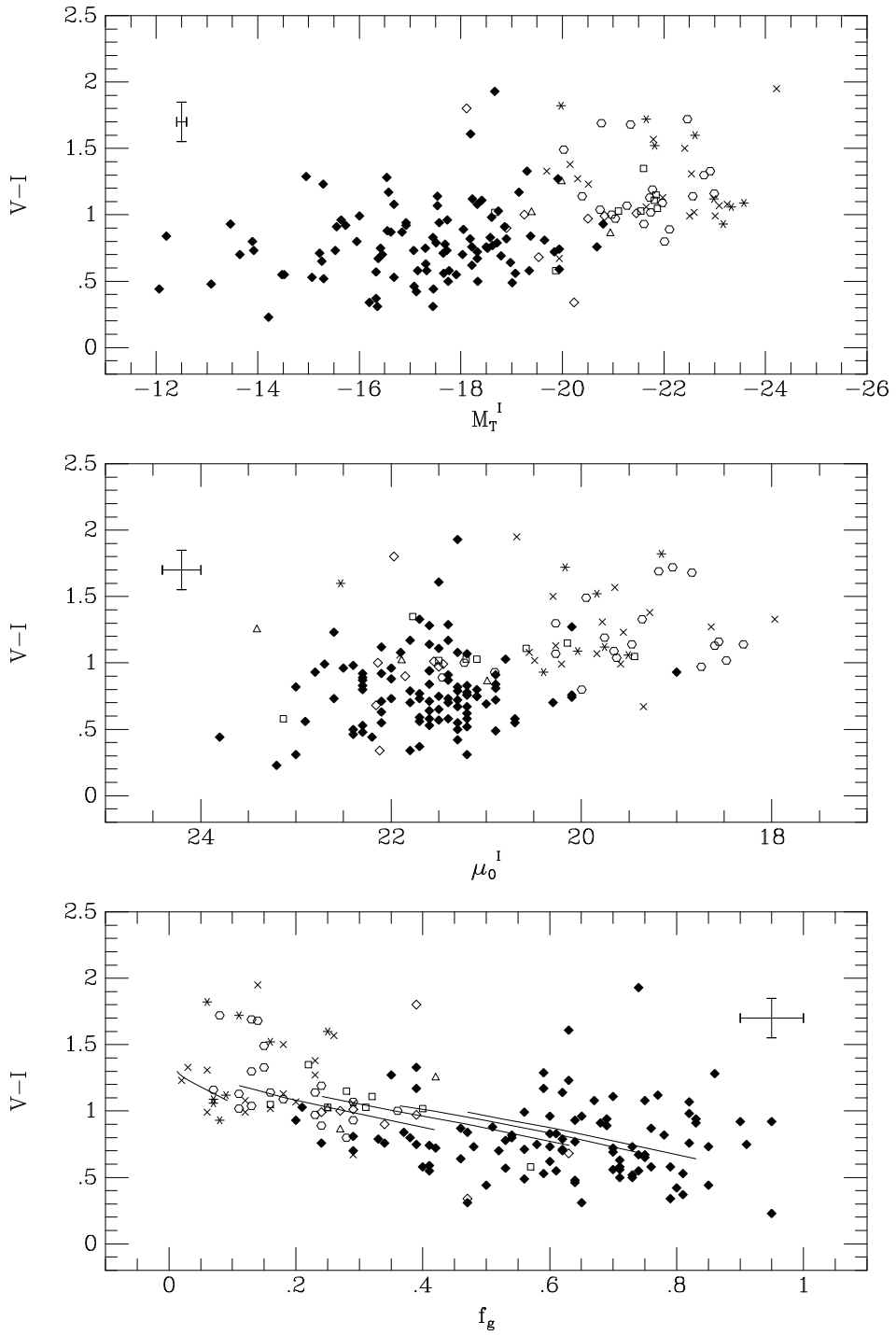


Fig. 6.—  $V - I$  color versus total luminosity ( $M_T^I$ ), central surface brightness ( $\mu_0^I$ ) and gas fraction ( $f_g$ ). The LSB dwarfs continue the sequence defined by ordinary spirals of fainter luminosities, higher gas fractions and lower surface brightnesses with bluer colors. The models of Boissier & Prantzos are shown in the bottom panel were high  $\lambda$  (LSB) are to the right. Symbols are the same as Figure 5.

changes due to short bursts of star formation.

McGaugh and de Blok found a strong correlation between color and magnitude or surface brightness; however, despite the tendency for LSB galaxies to have blue optical colors, there is no direct correlation between  $V - I$  and  $M_T^I$  or  $\mu_o$  for the LSB dwarf sample. On the other hand, the  $V - I, f_g$  relationship for LSB dwarfs is a clear extension of the disk relationships from MdB. Interpretation of this trend is problematic. Natively, one might expect that high gas mass fraction galaxies to have red colors reflecting their low rates gas mass conversion into stellar mass. The Boissier & Prantzos models are shown in the bottom panel of Figure 6 and correctly predict the decrease in color with increasing gas fraction. This would seem to confirm several of the characteristics to the high  $\lambda$  models, such as a rising star formation rate and slow chemical enrichment.

Also visible in Figure 6 is that the dwarfs with the highest gas fractions have the bluest colors. Blue colors have always been an enigma in the understanding of LSB stellar populations. In general, the cause of the bluer colors, compared to HSB galaxies, can either be 1) low mean metallicity, 2) younger mean age or 3) recent burst of star formation and, of course, some combination of the three. For example, van den Hoek *et al.* (2000) are able to reproduce the colors and gas fractions of LSB disks using an exponentially decreasing star formation model which is consistent with measured [O/H] values for their sample. However, they are unable to fit the bluest, dwarf LSB galaxies in their sample without an additional light contribution from a younger stellar population.

Considering metallicity effects first, LSB galaxies are known to have lower metallicities than HSB galaxies based on O[III] measurements of H II regions (McGaugh 1994, van Zee, Haynes & Salzer 1997). These values range from 1/3 to 1/20 solar, which corresponds to [Fe/H] of  $-0.4$  and  $-1.3$  dex. While  $V - I$  colors are not as sensitive to metallicity changes as color indices such as  $B - V$ , a shift in 1.0 dex in [Fe/H] will produce a change in 0.2 to the  $V - I$  colors (Bruzual & Charlot 2000). Thus, some of the blueward slope in top panel of Figure 6 is due to a decreasing mean metallicity from approximately solar at high masses to 1/25 solar at the faint end (Zaritsky 1993).

In order to examine the effects of metallicity, we have adapted the multi-metallicity models for dwarf ellipticals from Rakos *et al.* (2000) to the color-magnitude relation in Figure 6. These models combine the metallicity distribution given by the Kodama & Arimoto (1997) infall simulations with the single burst photometric models of Bruzual & Charlot (2000). For each metallicity bin in the Kodama & Arimoto model, the fraction of stars are calculated and the flux, plus color, are determined from the Bruzual and Charlot (2000) SSP's. Then, the total integrated color of a galaxy is calculated by summing the luminosity of each metallicity bin population. To simulate the change of metallicity with mass, the shape of the Kodama metallicity distribution is held fixed but the peak [Fe/H] is compressed to lower values but constant fractions. This procedure successfully produces the correct slope and zeropoints to the color-magnitude relation for ellipticals (see Rakos *et al.* 2000 for a fuller discussion).

The resulting mass-metallicity relation for a 13 Gyr population, converted into  $I$  band magnitudes and  $V - I$  color, is shown in the top panel of Figure 7. The model fits the blue edge of the de Jong disk galaxies fairly well and is, of course, the mass-metallicity relation for spirals documented by Zaritsky, Kennicutt & Huchra (1994). The number of disks galaxies above the 13 Gyr line probably represents systems with reddening due to dust. We also note that few LSB dwarfs display an indication of reddening, where the reddest LSB dwarfs are similar in  $V - I$  color to dwarf ellipticals. This observation is in agreement with their lack of IRAS detection (Schombert *et al.* 1990) and van den Hoek *et al.* (2000) also rule out any significant extinction by dust in high gas fraction LSB galaxies.

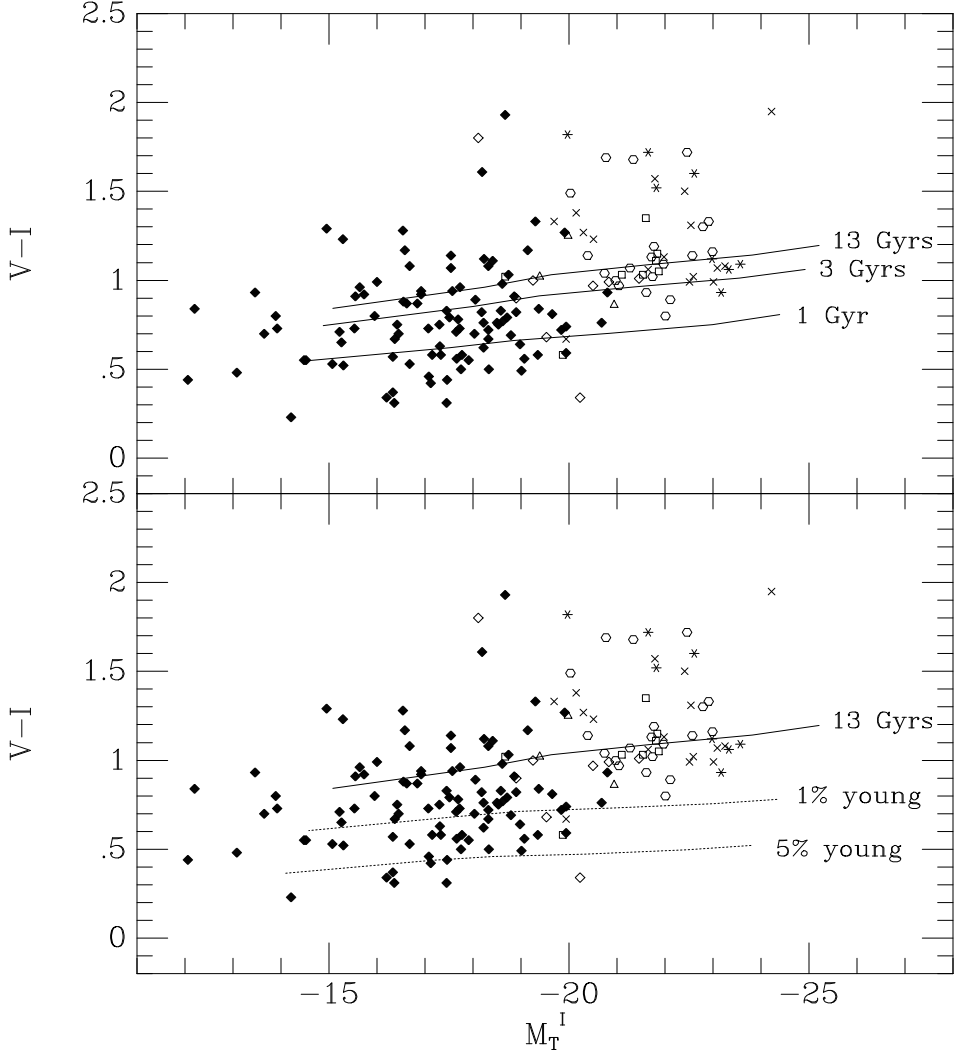


Fig. 7.—  $V - I$  color versus total luminosity ( $M_T^I$ ). Symbols are the same as Figure 6. The top panel displays the multi-metallicity models of Rakos *et al.* (2000) using the Bruzual & Charlot (2000) SED's to convert to  $V - I$  colors. Three population ages are shown; 13, 3 and 1 Gyrs. A majority of LSB dwarfs have mean  $V - I$  colors which concur with mean ages at least 10 Gyrs less than normal ellipticals. The bottom panel displays two ‘frosting’ models where a fraction of a recent (100 Myr) population is added to a 13 Gyrs population. While only a 1% burst is required to match the colors of LSB dwarfs, this population would contribute 40% of the total light of the galaxy and eliminate its LSB appearance. Symbols are the same as Figure 5.

While the color-magnitude relation works well for LSB disks, HSB spirals and ellipticals, a majority of the LSB dwarf sample continue to have  $V - I$  colors too blue for the expectation from their metallicities. Of course, it is possible that the stellar population, that produces the optical luminosity, has a much lower mean metallicity than the values measured from nebular spectroscopy since those values represent the current metallicity of ongoing star formation. However, the multi-metallicity models take into account the contribution from metal-poor stars and to achieve the  $V - I$  colors observed for LSB dwarfs would require a contrived evolutionary history such that a majority of the stars have globular cluster metallicities with a recent, and abrupt, rise in the mean metallicity to match H II region spectroscopy. Dominance of a globular cluster metallicity population certainly can not be the case in all LSB dwarfs since the galaxies with the highest  $V - I$  values (the ‘red’ edge in Figure 7) follow the same mass-metallicity relation as disk and dwarf ellipticals (predicting mean metallicities of  $[\text{Fe}/\text{H}] = -0.8$  from the models). If the blueward dwarfs are due to metallicity effects, then the mass-metallicity sequence breaks down below  $M_T^I = -20$ , which is not indicated by LSB nebular spectroscopy (Bell *et al.* 2000).

An alternative explanation is that the spread in  $V - I$  color is due to changes in the mean age of the stellar population in LSB dwarfs. To test the effects of age, we have recomputed the luminosities and colors of the multi-metallicity models for ages of 1 and 3 Gyrs (shown in Figure 7) where an initial burst of star formation is assumed with a duration that is less than 0.1 Gyrs. The  $V - I$  colors evolve quickly reaching the red edge in only 5 to 6 Gyrs. If mean age is responsible for the bluer  $V - I$  colors, then an age between 1 and 3 Gyrs is indicated. This, of course, does not imply that LSB dwarfs formed less than 4 Gyrs ago since a young mean age can be achieved through a number of scenarios. For example, the Boissier & Prantzos models predict an increasing star formation rate with time in their high  $\lambda$ , low mass simulations. With e-folding timescales between 7 and 11 Gyrs (as indicated by Figure 7), then a majority of the luminosity in LSB dwarfs originates from stars with ages less than 3 Gyrs even though there will exist stars dating back to the epoch of galaxy formation.

A younger mean age can also be produced by a burst of recent star formation on top of an underlying old population. Recent star formation can be tested for using so-called frosting models, where some percentage of young stars is added to a 13 Gyr population. The bottom panel of Figure 7 displays the effects of adding 1% and 5% of a 100 Myr population to the 13 Gyrs mass-metallicity sequence. While a 5% young population is sufficient to match the  $V - I$  colors of the LSB dwarfs in the color-magnitude diagram, a star formation burst of this magnitude is inconsistent with other properties of LSB galaxies. For example, the burst population in a 1% population contributes 40% of the total light of the galaxy and in a 5% population this percentage rises to 80% of the total light. Given the slow rotation velocities for dwarfs, this young, bright population would maintain a tight spatial correlation producing many high surface brightness knots, in contradiction with the visual appearance of the LSB dwarfs. In order to maintain a low stellar density and the lack of color gradient (Pildis, Schombert & Eder 1997), the young population would have to be evenly distributed instead of in cloud complexes, which is style of star formation currently undocumented in extragalactic studies. In addition, even if the recent burst were spread evenly within the LSB dwarf, the burst strength is inconsistent with the current metallicities and gas fractions.

Lastly, the difference in  $V - I$  colors between LSB dwarfs and disks may be due to the fact that disk systems have high amounts of dust extinction. Clearly some of the disk colors in Figure 6 are reddened, particularly the objects between  $V - I = 1.5$  and 2. Half of the early-type disks have  $V - I$  colors greater than 1.2, the red edge for the LSB dwarfs, while the rest of the same appear to be less effected by extinction effects and with a blue edge to the disk sample near  $V - I = 1$ . Tully *et al.* (1998) finds that, in the extreme case of a sample of edge-on galaxies, extinction at  $I$  can reach 1 mag, which would correspond to 0.3 in  $V - I$ .

However, studies of overlapping pairs of ellipticals and late-type galaxies by Domingue, Keel & White (2000) find only modest amounts of extinction. The correlation of color-magnitude for disk galaxies near  $V - I = 1$  would argue that we are observing a majority of the optical luminosity in disk galaxies unless extinction effects conspire to redden the mean colors into this linear relationship.

#### 4. CONCLUSIONS

In this study we have isolated the optical and HI properties of a sample of LSB dwarfs galaxies in order to study the relationship between gas fraction and star formation history. Our primary results can be summarized as the following:

- (1) Objects selected by irregular dwarf-like morphology (to be distinguished from irregular tidal morphology) do indeed define a sample of galaxies that are faint, small and low mass (Pildis, Schombert & Eder 1997). However, no single characteristic defines a galaxy as uniquely dwarf or giant. There is a continuum of optical properties, such as central surface brightness, luminosity and scale length, over the range of galaxy Hubble types (Figure 1).
- (2) The distribution of HI mass is such that the typical LSB dwarf has less than  $5 \times 10^9 M_{\odot}$  of neutral gas (Figure 2). Over 1/3 of the dwarfs in this sample have HI mass less than  $5 \times 10^8 M_{\odot}$ . A galaxy defined by irregular morphology will not only be dwarf in size and luminosity, but also by HI mass and dynamical mass (Eder & Schombert 2000).
- (3) There is a relationship between stellar mass and gas mass for both dwarf and disk galaxies (Figure 3). However, the relation for dwarfs is much shallower than the relation for disks implying that disks have been more efficient at converting gas into stars in the past (Bell & de Jong 2000). This is in line with the more ordered appearance for disks versus the chaotic structure for dwarfs, but this conclusion is dependent on only small variations in  $M/L$  between late-type disks and dwarfs, which may not be the case (see Bell & de Jong 2001).
- (4) LSB dwarfs typically have much higher gas fractions (the ratio of stellar to gas mass) than disk galaxies (Figure 2). Many of the simple correlations in disk galaxies between gas fraction and luminosity or surface brightness are weaker in the dwarf realm. LSB dwarfs with the bluest colors have the highest gas fractions (Figure 6).

The gas mass fraction of a galaxy must be a key parameter to its evolutionary path since the pattern, duration and strength of star formation are directly determined by the amount of fuel available to support star formation. Disk galaxies, with red underlying stellar populations and low gas fractions, suggests a star formation history that involves a constant, or declining, star formation at relatively high rates (Bell & de Jong 2000, van den Hoek *et al.* 2000). Under this scenario, the gas fraction becomes a gauge of integrated past conversion of gas into stars. Thus, the Hubble sequence is a progression of star formation rates, where Sa's had the highest rates and, in the present epoch, the lowest gas fraction and Sc's have had lower rates and maintained higher gas fractions.

For LSB dwarfs, their global characteristics are the reverse to ordinary spirals. They have very little in the way of a stellar population and a majority of their baryonic mass is in the form of neutral hydrogen. The stellar population that does exist is very low in surface density and very blue based on their  $V - I$

colors (Pildis, Schombert & Eder 1997). Using the prescription from van Zee, Haynes & Salzer (1997), their integrated past star formation rate is typically less than  $0.1 M_{\odot} \text{ yr}^{-1}$  and  $\text{H}\alpha$  imaging of a few LSB dwarfs indicates current star formation rates of  $0.01 M_{\odot} \text{ yr}^{-1}$ . On the other hand, their gas mass fractions are very high, greater on average than the typical Sc galaxy. Combining their current colors and star formation properties with the knowledge that their metallicities are low (1/3 to 1/20 of solar), LSB dwarfs must represent unevolved systems that have consumed very little of their original gas supply in agreement with van Zee, Haynes & Salzer (1997) study of gas-rich dwarfs.

Our comparison to simple photometric/gas consumption models presented in §3.3 (displayed in Figure 5) provides the key difference in the characteristics of dwarfs and disks. Disk galaxies, over a range of central surface brightnesses, have used a significant fraction of their gas to produce stars (see also Bell & de Jong 2000). They have short star formation e-folding times, but display relatively old mean stellar ages reflecting a long history of substantial star formation. Dwarfs, on the other hand, have consumed very little of their gas due to their long star formation timescales, and their current, dominant stellar population has a very young age (less than 5 Gyr's on average).

Young mean age, either by constant or increasing star formation, appears to be most likely solution to the optical colors presented in Figure 7. With the levels of star formation deduced for the integrated past or for the observed current, is difficult to envision star formation, spread evenly in time and spatial position. More likely, star formation in LSB dwarfs proceeds in weak bursts that percolates over the spatial extent of the galaxies with each event consuming only a small fraction of the local HI gas mass. This hypothesis of weak bursts on top of a very LSB stellar population is in agreement with  $\text{H}\alpha$  studies of LSB galaxies (Walter & Brinks 1999) where star formation traces both the gas and the surface brightness and also in agreement with the conclusions of Bell *et al.* (2000), who found a strong correlations with an LSB galaxies star formation history and its local surface density.

We conclude with a comment on the differences between LSB dwarf galaxies and LSB disk galaxies. The star formation history of LSB disk galaxies has recently been explored by both Bell *et al.* (2000) and van den Hoek *et al.* (2000). The study of LSB disks by van den Hoek *et al.* found that they have gas fractions lower than the LSB dwarfs presented here, but still higher than HSB disk galaxies (e.g.,  $f_g$  around 0.5). They find that exponentially decreasing SFR models are a good match to most of LSB disk properties; however, weak bursts are indicated for the bluest systems. Bell *et al.* find similar results with the additional correlation between local surface brightness (mass density) and past plus current star formation rate. Both studies find that LSB disks are lower in mean age than HSB disks, mostly due to the more rapid build-up of a stellar population in HSB with higher past rates of star formation. In other words, a higher surface brightness system has more old stars per  $\text{pc}^{-2}$  and, thus, its calculated mean age from model comparison is older. LSB dwarfs have many characteristics in common with LSB disks, but the star formation history can not be as smooth and uniform as proposed by Bell *et al.* and van den Hoek *et al.* for LSB disks. The disk correlations found by MdB are much weaker for LSB dwarfs signaling a difference in the style of star formation even within the class of LSB galaxies. We suspect that the dynamical state of disks versus dwarfs is responsible for the changes seen in their stellar and gas properties as a galaxy transitions from ordered rotation to the more turbulence dominated solid-body rotation found in dwarfs (see van Zee, Haynes & Salzer 1997). However, that conclusion remains in question until high resolution HI mapping of LSB dwarfs are presented in a future paper.

We wish to thank the generous support of the Arecibo Observatory for the allocation of time to search for HI emission from the candidate dwarf galaxies and MDM Observatory in carrying out the photometry portion

of this program. This work is based on photographic plates obtained at the Palomar Observatory 48-inch Oschin Telescope for the Second Palomar Observatory Sky Survey which was funded by the Eastman Kodak Company, the National Geographic Society, the Samuel Oschin Foundation, the Alfred Sloan Foundation, the National Science Foundation and the National Aeronautics and Space Administration.

## REFERENCES

Ashman, K. 1992, PASP, 104, 1109

Baugh, C., Cole, S. & Frenk, C. 1996, MNRAS, 283, 1361

Bell, E., Barnaby, D., Bower, R., de Jong, R., Harper, D., Hereld, M., Loewenstein, R. & Rauscher, B. 2000, MNRAS, 312, 470

Bell, E. & de Jong, R. 2001, astro-ph/0011493

Bell, E. & de Jong, R. 2000, MNRAS, 312, 497

de Blok, W., McGaugh, S. & van der Hulst, T. 1996, MNRAS, 283, 18

de Blok, W. & van der Hulst, J. 1998, A&A, 336, 49

Boissier, S. & Prantzos, N. 2000, MNRAS, 312, 398 (BP)

Bothun, G., Eriksen, J. & Schombert, J. 1994, AJ, 108, 913

Bottema, R. 1993, A&A, 275, 16

Bruzual, G. & Charlot, S. 1993, ApJ, 405, 538

Bruzual, A. & Charlot, S. 2000, private communication

Carignan, C. & Purton, C. 1998, ApJ, 506, 125

Courteau, S. 1996, ApJS, 103, 363

Dekel, A. & Silk, J. 1986, ApJ, 303, 39

Dohm-Palmer, R., Skillman, E., Gallagher, J., Tolstoy, E., Mateo, M., Dufour, R., Saha, A., Hoessel, J. & Chiosi, C. 1998, AJ, 116, 1227

Domingue, D., Keel, W. & White, R. 2000, ApJ, 545, 171

Driver, S., Windhorst, R. & Griffiths, R. 1995, ApJ453, 48

Driver, S. & Cross, N. 2000, astro-ph/0004201

Eder, J., Oemler, A., Schombert, J. & Dekel, A. 1989, ApJ, 340, 29

Eder, J. & Schombert, J. 2000, ApJS, 131, 47

Firmani, C. & Tutkov, A. 1992, A&A, 264, 37

Gerritsen, J. & de Blok, W. 1999, A&A, 342, 655

Giovanelli, R. & Haynes, M. 1988, in *Galactic and Extragalactic Radio Astronomy*, (New York:Springer-Verlag), p. 522

Holmberg, E 1950, *Medd. Lund. Obs. Ser. 2*, no. 128

Hunter, D. & Gallagher, J. 1986, PASP, 98, 5

Impey, C., Sprayberry, D., Irwin, M. & Bothun, G. 1996, ApJS, 105 209

de Jong, R. 1996, A&A, 313, 45  
Kennicutt, R. 1998, ApJ, 498, 541  
Kodama, T. & Arimoto, N. 1997, A&A, 320, 41  
Lake, G. 1990, ApJ, 364, 1  
Matthews, L., van Driel, W. & Gallagher, J. 1998, AJ, 116, 1169  
MacLow, M. & Ferrara, A., ApJ, 513, 142  
McGaugh, S. 1994, ApJ, 426, 135  
McGaugh, S. & Bothun, G. 1994, AJ, 107, 530  
McGaugh, S., Schombert, J. & Bothun, G. 1995, AJ, 109, 2019  
McGaugh, S. & de Blok, W. 1997, ApJ, 481, 689  
McGaugh, S., Schombert, J., Bothun, G. & de Blok, W. 2000, ApJ, in press  
Mihos, C., Spaans, M. & McGaugh, S. 1999, ApJ, 515, 89  
Mo, H., Mao, S. & White, S. 1998, MNRAS, 295, 319  
Patterson, R. & Thuau, T. 1996, ApJS, 107, 103  
Pildis, R., Schombert, J. & Eder, J. 1997, ApJ, 481, 157  
O'Neil, K., Bothun, G., Schombert, J., Cornell, M. & Impey, C. 1997, AJ, 114, 2448  
Rakos, K., Odell, A. & Schombert, J. 1997, ApJ, 490, 194  
Rakos, K., Schombert, J., Maitzen, H., Prugovecki, S. & Odell, A. 2000, AJ, in press.  
Reid, I., Brewer, C., Brucato, R., McKinley, W., Maury, A., Mendenhall, D., Mould, J., Mueller, J., Neugebauer, G., Phinney, J., Sargent, W., Schombert, J. & Thicksten, R. 1991, PASP, 103, 661  
Sandage, A. & Binggeli, B. 1984, AJ, 89, 919  
Schade, D., Lilly, S., Le Fevre, O., Hammer, F. & Crampton, D. 1996, ApJ, 464, 79  
Schneider, S., Spitzak, J. & Rosenberg, J. 1998, ApJ, 507, 9  
Schneider, S. & Schombert, J. 2000, ApJ, 530, 286  
Schombert, J. & Bothun, G. 1988, AJ, 95, 1389  
Schombert, J., Bothun, G., Impey, C. & Mundy, L. 1990, AJ, 100, 1523  
Schombert, J., Bothun, G., Schneider, S. & McGaugh, S. 1992, AJ, 103, 1107  
Schombert, J., Pildis, R., Eder, J. & Oemler, A. 1995, AJ, 110, 2067  
Schombert, J., Pildis, R. & Eder, J. 1997, ApJS, 111, 233  
Scoville, N., Sargent, A., Sanders, D. & Soifer, B. 1991, ApJ, 366, L5  
Tammann, G. 1980, *Dwarf Galaxies*, ed. M. Tarenghi and K. Kjar (Geneva:ESO), 3  
Tully, R., Pierce, M., Huang, J., Saunders, W., Verheijen, M. & Witchalls, P. 1998, AJ, 115, 2274  
de Vaucouleurs, G. 1959, *Handbuch Phys.*, 53, 275  
Walter, F. & Brinks, E. 1999, AJ, 118, 273  
Worthey, G. 1994, ApJS, 95, 107  
Young, J. & Knezeck, P. 1989, ApJ, 347, 55

Zaritsky, D. 1993, PASP, 105, 1006

Zaritsky, D., Kennicutt, R. & Huchra, J. 1994, ApJ, 420, 87

van den Hoek, L., de Blok, W., van der Hulst, J. & de Jong, T. 2000, A&A, 357, 397

van Zee, L., Haynes, M. & Salzer, J. 1997, AJ, 114, 2479

Zwaan, M., Briggs, F., Sprayberry, D. & Sorar, E. 1997, ApJ, 490, 173